

## Influence of annealing on stimulated emission in ZnO nanorods

W. M. Kwok

*Department of Chemistry, The University of Hong Kong, Pokfulam Road, Hong Kong*

Aleksandra B. Djurišić<sup>a)</sup>

*Department of Physics, The University of Hong Kong, Pokfulam Road, Hong Kong*

Yu Hang Leung

*Department of Chemistry, The University of Hong Kong, Pokfulam Road, Hong Kong*

D. Li and K. H. Tam

*Department of Physics, The University of Hong Kong, Pokfulam Road, Hong Kong*

D. L. Phillips and W. K. Chan

*Department of Chemistry, The University of Hong Kong, Pokfulam Road, Hong Kong*

(Received 14 August 2006; accepted 21 September 2006; published online 2 November 2006)

Vertically aligned ZnO nanorod arrays with rod lengths in the range of 200–1500 nm were fabricated by a hydrothermal method. No stimulated emission was observed in as grown nanorods. Annealing of the rods in forming gas and oxygen significantly affected their optical properties and enabled the achievement of stimulated emission. The lowest lasing threshold and defect emission as well as the longest spontaneous emission decay times were obtained for nanorods annealed in oxygen flow. This indicates that interstitial oxygen, which is commonly assumed to be the cause of yellow-green defect emission, is not the dominant defect in hydrothermally grown nanorods. © 2006 American Institute of Physics. [DOI: 10.1063/1.2378560]

Stimulated emission in ZnO nanostructures has been extensively studied.<sup>1–11</sup> However, a very wide range of lasing thresholds has been reported in the literature, and different feedback mechanisms (random lasing versus nanostructures as Fabry-Pérot cavities) have been proposed.<sup>1</sup> Different types of cavities have been reported for ZnO nanostructures. In straight nanostructures such as nanowires and nanoribbons, the cavity is formed between two crystal facets.<sup>10</sup> Stimulated emission can also be observed in nanostructures where one facet has lower reflectivity, such as tetrapods<sup>2,11</sup> and nanoribbon/combs.<sup>2</sup> In addition, whispering gallery mode lasing has been observed in ZnO nanonails.<sup>3</sup> On the other hand, stimulated emission in ZnO nanowires with random orientations was attributed to a random lasing phenomenon.<sup>6</sup> It has also been shown that, while stimulated emission is easily achievable in nanowires with random orientations, no stimulated emission is found in well-aligned nanowires.<sup>6</sup> However, lasing in aligned arrays of ZnO nanorods has been previously achieved.<sup>4,8</sup>

In addition to the alignment, size, and shape of the nanostructures, the crystal quality of the ZnO structures is another factor which affects the achievement of stimulated emission.<sup>5,9</sup> In general, ZnO nanostructures fabricated by a hydrothermal method are expected to have a larger number of defects due to a low growth temperature (<100 °C). However, the hydrothermal method<sup>12–14</sup> is of considerable interest for practical applications. Stimulated emission has been previously demonstrated in nanorods grown by the hydrothermal method.<sup>2,8</sup> In both cases, ZnO nanoparticles were used as a seed, but due to the different nanoparticle seed sizes, the degree of vertical alignment was different. It has been reported that the use of seeds derived from zinc acetate solution on the substrate results in an improved vertical ori-

entation of the nanorods.<sup>12</sup> The aligned nanorods also have higher UV to visible emission ratios compared to those prepared with ZnO nanoparticle seeds. Therefore, we studied the photoluminescence of aligned ZnO nanorod arrays having different rod lengths. Up to 1.5 μm, no stimulated emission is observed in as grown nanorods. However, annealing in oxygen or forming gas enables the achievement of stimulated emission in the 1.4–1.5 μm long rods. The rods annealed in oxygen had lower defect emission and lower lasing threshold, which is in contradiction with the hypothesis that defects related to excess oxygen<sup>13,14</sup> are prevalent in hydrothermally grown samples.

The ZnO nanorods were prepared by a hydrothermal method<sup>12–14</sup> from an aqueous solution of zinc nitrate hydrate polyethyleneimine and hexamethylenetetramine, as described previously.<sup>13</sup> The seed layer on Si substrates was prepared from the zinc acetate solution.<sup>12</sup> The rod length was varied by repeating hydrothermal growth cycles by placing the rods into freshly prepared solutions. The morphology before and after annealing was examined using a Leo 1530 field emission scanning electron microscope (SEM) and transmission electron microscopy (TEM) using Phillips Tecnai 20 and JEOL 2010F TEM. The rods were annealed in a tube furnace at 600 °C in the flow of oxygen or forming gas (90% N<sub>2</sub>/10% H<sub>2</sub>) at a flow rate of 0.1 l/min. and a pressure of 1 Torr. cw photoluminescence over a wide spectral range was excited by a He–Cd laser (325 nm) and recorded by a PDA-512-USB (Control Development Inc.) fiber optic spectrometer. Time-resolved photoluminescence (TRPL) was measured by using the Kerr gated fluorescence technique.<sup>15</sup> For the TRPL and time-integrated photoluminescence measurements, the samples were excited by a 267 nm laser pulse from a Ti:sapphire regenerative amplifier laser system focused to a spot size of 300 μm diameter. The rod density per spot size was of the order of several millions. The pulse

<sup>a)</sup>FAX: +852 2559 9152; electronic mail: dalek@hkusua.hku.hk

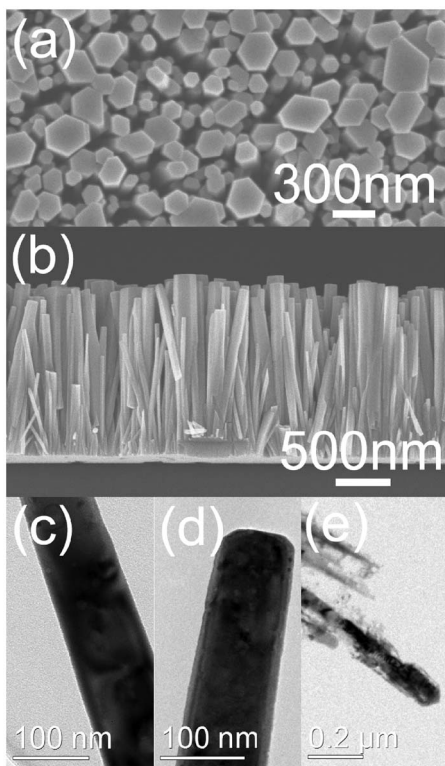


FIG. 1. SEM images of ZnO nanorods: (a) top view and (b) side view. TEM images of Zn nanorods (c) as grown, (d) annealed in  $O_2$ , and (e) annealed in forming gas.

duration was about 250 fs, and the instrument response time was about 1 ps.

Figure 1 shows the SEM and TEM images of the hydrothermally grown rods. Figures 1(a) and 1(b) show the top and side views of the rods obtained after repeating the cycle of hydrothermal growth six times. The rod lengths for one growth cycle were in the range of 200–300 nm, and the diameters were in the range of 25–50 nm. Both the diameters and lengths increase with increasing number of growth cycles, so that after repeating the growth six times rods with diameters in the range of 100–200 nm and length in the range of 1400–1500 nm are obtained. Representative TEM images of as grown and annealed rods are shown in Figs. 1(c)–1(e). The annealing in oxygen does not result in any obvious change of the morphology, while annealing in forming gas leads to the reduction in the rod diameter and deterioration in the surface quality of the rods.

Room temperature PL spectra from the  $\sim 1.5 \mu\text{m}$  long rods before and after annealing are shown in Fig. 2. Similar changes are observed for all rod lengths, except for the fact that UV to visible emission ratio appeared to be dependent on the rod length, which is likely due to different surface-to-volume ratios of the rods. As grown rods exhibit yellow-green emission centered at  $\sim 580 \text{ nm}$ , commonly observed in hydrothermally grown ZnO nanorods.<sup>13,14,16</sup> Yellow emission has been previously attributed to oxygen interstitial defects.<sup>13,14</sup> However, yellow-green emission has also been attributed to the presence of OH groups.<sup>17,18</sup> Since the yellow emission is absent after annealing at 200 °C and above, it likely originates from the presence of OH groups whose desorption temperature is 150 °C.<sup>18</sup> After annealing in oxygen, a weak peak in the red spectral region ( $\sim 670 \text{ nm}$ ) can be observed, while annealing in forming gas produces two

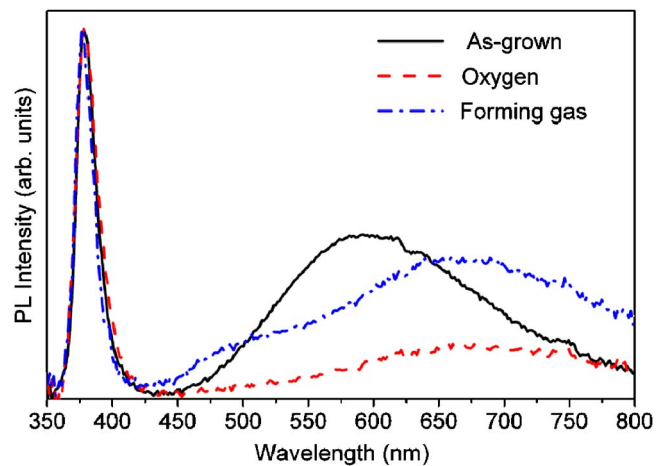


FIG. 2. (Color online) Room temperature photoluminescence of ZnO nanorods annealed under different conditions.

peaks, one in the green ( $\sim 500 \text{ nm}$ ) and one in the red ( $\sim 670 \text{ nm}$ ) spectral regions. It has been shown that the green, yellow, and orange-red emissions have different origins.<sup>16</sup> The green luminescence is associated with surface defects,<sup>16</sup> so that the appearance of the green emission peak after obvious surface damage caused by forming gas annealing is expected. As for the origin of red emission, it is typically attributed to defects associated with excess oxygen.<sup>16</sup> However, this emission persists both after annealing in reducing (forming gas) and oxidizing (oxygen) environments and at temperatures as high as 600 °C. This indicates that defect complexes rather than single point defects, which are expected to be mobile at temperatures below 600 °C and thus would anneal out, are responsible for this emission. However, the exact chemical origin of these defect complexes requires further study.

The stimulated emission could be achieved in ZnO nanorods grown by a hydrothermal method with nanoparticle seeds.<sup>2</sup> The obtained threshold was relatively high,  $\sim 480 \mu\text{J}/\text{cm}^2$ , while the mode width was 0.6–0.9 nm.<sup>2</sup> Choy *et al.*<sup>8</sup> also reported stimulated emission in hydrothermally grown ZnO nanorods with nanoparticle seeds, with a larger rod size ( $\sim 100 \text{ nm}$  diameter) and a lower threshold of  $\sim 140 \mu\text{J}/\text{cm}^2$ . However, in spite of indications of the improved optical quality of ZnO nanorods grown with a zinc acetate seed based on higher UV to visible emission ratio, no stimulated emission is observed in as grown nanorods for all lengths up to  $\sim 1.5 \mu\text{m}$ . For the  $1.5 \mu\text{m}$  long nanorods, lasing is observed only after annealing. The emission spectra after annealing for different excitation powers and the dependence of the emission intensity on the pump fluence are shown in Fig. 3. For both annealing atmospheres, a single mode at  $\sim 385 \text{ nm}$  with  $\sim 0.6$  full width at half maximum (FWHM) appears. The lasing threshold is higher in the case of samples annealed in forming gas (on average  $\sim 48 \mu\text{J}/\text{cm}^2$  for oxygen annealing and  $56 \mu\text{J}/\text{cm}^2$  for forming gas annealing), but it is considerably lower than that in ZnO nanorods grown with a nanoparticle seed.<sup>2</sup> The photoluminescence decay curves monitored at 380 and 385 nm are shown in Fig. 4. In all cases, the spontaneous emission exhibits biexponential decays with decay constants of  $\tau_1 = 8 \text{ ps}$  and  $\tau_2 = 40 \text{ ps}$  for as grown nanorods,  $\tau_1 = 8 \text{ ps}$  and  $\tau_2 = 44 \text{ ps}$  for nanorods annealed in forming gas, and  $\tau_1 = 20 \text{ ps}$  and  $\tau_2 = 67 \text{ ps}$  for nanorods annealed in oxygen. This

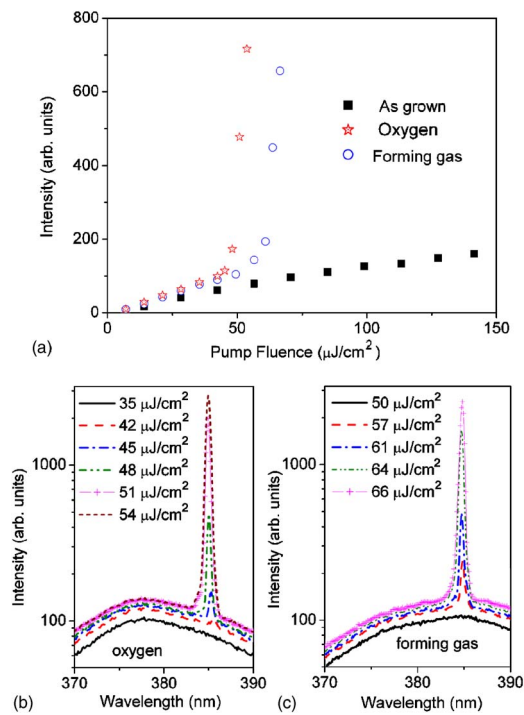


FIG. 3. (Color online) (a) Emission intensity vs pump fluence for ZnO nanorods. Time-integrated photoluminescence from ZnO nanorods annealed in (b) oxygen and (c) forming gas.

indicates the reduction of nonradiative defect concentration after annealing in oxygen flow. Stimulated emission had similar decay times for both annealing atmospheres and a short decay time  $<1$  ps, similar to nanorods grown with nanoparticle seeds, which exhibited decay times of 4 ps and decay time of  $\sim 1$  ps.<sup>2</sup>

It should be noted that the stimulated emission after annealing is observed only in the largest rods. Rods obtained using fewer growth cycles do not exhibit stimulated emission reproducibly at a number of places in the samples. Since the threshold gain is inversely proportional to the nanostructure length,<sup>1,2,10,11</sup> stimulated emission is typically more readily achievable in longer nanostructures, although stimulated emission in  $\sim 300$  nm long isolated nanorods with pyramidal tops has been reported.<sup>7</sup> However, both rod diameter and length change with the number of growth cycles. The larger

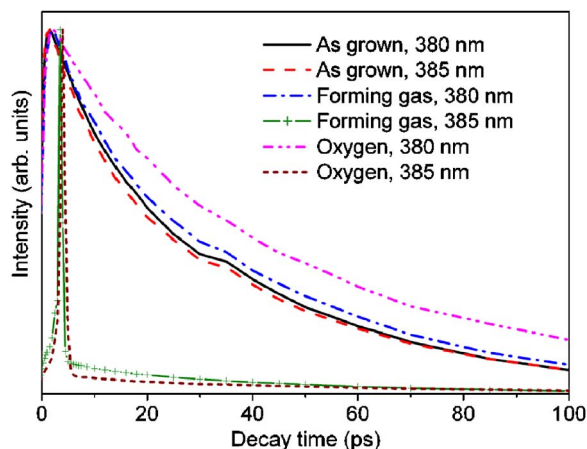


FIG. 4. (Color online) Photoluminescence decay curves of ZnO nanorods annealed under different conditions monitored at 380 and 385 nm.

diameter of the nanorods as a requirement for achievement of stimulated emission has been recognized.<sup>4,5,10,11</sup> For nanowires with a radius of 50 nm,  $<25\%$  of the field intensity is guided within the nanowire, while for thicker wires with a radius of 100 nm, the field percentage within the wire is  $>90\%$ .<sup>11</sup> Thus, the absence of lasing in nanorods grown for fewer growth cycles is likely due to their smaller diameter. The lasing mode observed likely corresponds to a fundamental longitudinal mode since the behaviors of the samples annealed in oxygen and those annealed in forming gas are very similar indicating that damage to the side surfaces after forming gas annealing does not affect lasing. This is further supported by the fact that only a single stimulated emission mode is observed for a range of excitation powers. For a cavity with  $1.5 \mu\text{m}$  length, using refractive index estimates given in Ref. 11, the mode spacing is expected to be  $\sim 14.5$  nm, so that only one longitudinal lasing mode can be supported. For very high excitation powers, additional modes can be observed.

To summarize, vertically aligned arrays of ZnO nanorods were fabricated by a hydrothermal method. Unlike the samples with inferior alignment, no stimulated emission was found in as grown nanorods with lengths up to  $1.5 \mu\text{m}$ . However, stimulated emission is obtained after both annealing in oxygen and forming gas in spite of the different effects of those annealing environments on rod morphology, defect emission, and PL decay times.

This work was supported by the Research Grants Council of Hong Kong (Project Nos. HKU 7008/04P, HKU 7019/04P, HKU 7010/05P, HKU 7029/06P, and HKU 1/01C)). Financial support from the Strategic Research Theme, University Development Fund, and Science Faculty Development Fund (University of Hong Kong) is also acknowledged.

<sup>1</sup>A. B. Djurišić and Y. H. Leung, *Small* **2**, 944 (2006).

<sup>2</sup>A. B. Djurišić, W. M. Kwok, Y. H. Leung, W. K. Chan, and D. L. Phillips, *J. Phys. Chem. B* **109**, 19228 (2005).

<sup>3</sup>D. Wang, H. W. Seo, C.-C. Tin, M. J. Bozack, J. R. Williams, M. Park, and Y. Tzeng, *J. Appl. Phys.* **99**, 093112 (2006).

<sup>4</sup>R. Hauschild, H. Lange, H. Priller, C. Klingshirm, R. Kling, A. Waag, H. J. Fan, M. Zacharias, and H. Kalt, *Phys. Status Solidi B* **243**, 853 (2006).

<sup>5</sup>A. N. Gruzintsev, A. N. Redkin, G. A. Emelchenko, C. Barthou, and P. Benalloui, *J. Opt. A, Pure Appl. Opt.* **8**, S148 (2006).

<sup>6</sup>H.-C. Hsu, C.-Y. Wu, and W.-F. Hsieh, *J. Appl. Phys.* **97**, 064315 (2005).

<sup>7</sup>T. Okada, K. Kawashima, and M. Ueda, *Appl. Phys. A: Mater. Sci. Process.* **81**, 907 (2005).

<sup>8</sup>J.-H. Choy, E.-S. Jang, J.-H. Won, J.-H. Chung, D.-J. Jang, and Y.-W. Kim, *Adv. Mater. (Weinheim, Ger.)* **15**, 1911 (2003).

<sup>9</sup>W. M. Kwok, A. B. Djurišić, Y. H. Leung, W. K. Chan, and D. L. Phillips, *Appl. Phys. Lett.* **87**, 223111 (2005).

<sup>10</sup>J. C. Johnson, H. Yan, P. Yang, and R. J. Saykally, *J. Phys. Chem. B* **107**, 8816 (2003).

<sup>11</sup>D. J. Sirbully, M. Law, H. Yan, and P. Yang, *J. Phys. Chem. B* **109**, 15190 (2005).

<sup>12</sup>L. E. Greene, M. Law, D. H. Tan, M. Montano, J. Goldberger, G. Somorjai, and P. Yang, *Nano Lett.* **5**, 1231 (2005).

<sup>13</sup>L. E. Greene, M. Law, J. Goldberger, F. Kim, J. C. Johnson, Y. Zhang, R. J. Saykally, and P. Yang, *Angew. Chem., Int. Ed.* **42**, 3031 (2003).

<sup>14</sup>D. Li, Y. H. Leung, A. B. Djurišić, Z. T. Liu, M. H. Xie, S. L. Shi, S. J. Xu, and W. K. Chan, *Appl. Phys. Lett.* **85**, 1601 (2004).

<sup>15</sup>C. Ma, W. M. Kwok, W. S. Chan, P. Zuo, J. T. W. Kan, P. H. Toy, and D. L. Phillips, *J. Am. Chem. Soc.* **127**, 1463 (2005).

<sup>16</sup>A. B. Djurišić, Y. H. Leung, K. H. Tam, L. Ding, W. K. Ge, H. Y. Chen, and S. Gwo, *Appl. Phys. Lett.* **88**, 103107 (2006).

<sup>17</sup>N. S. Norberg and D. R. Gamelin, *J. Phys. Chem. B* **109**, 20810 (2005).

<sup>18</sup>R. Xie, T. Sekiguchi, T. Ishigaki, N. Ohashi, D. Li, D. Yang, B. Liu, and Y. Bando, *Appl. Phys. Lett.* **88**, 134103 (2006).